Recent Applications of the Volterra Theory to Aeroelastic Phenomena

Walter A. Silva *
NASA Langley Research Center

Muhammad R. Hajj †
Virginia Polytechnic Institute and State University

Richard J. Prazenica ‡
University of Florida, Gainesville

The identification of nonlinear aeroelastic systems based on the Volterra theory of nonlinear systems is presented. Recent applications of the theory to problems in experimental aeroelasticity are reviewed. These results include the identification of aerodynamic impulse responses, the application of higher-order spectra (HOS) to wind-tunnel flutter data, and the identification of nonlinear aeroelastic phenomena from flight flutter test data of the Active Aeroelastic Wing (AAW) aircraft.

Introduction

The study of nonlinear systems is of great interest to scientists across a wide variety of disciplines.[1–9] Initiated, in some respects, by the seminal work of Poincare, the study of nonlinear systems experienced a rapid growth at the turn of the century and continues to grow as the fundamental concepts of nonlinear dynamics are applied to a wide range of problems. The field known as dynamical systems provides a unified interpretation of nonlinear dynamics based on topological concepts.[10–12] This mathematical interpretation of nonlinear dynamical processes provides a common language for the interpretation of nonlinear phenomena for scientists with diverse technical backgrounds.

Although dynamical system theories provide an important framework for the study of nonlinear systems, the complexity of a nonlinear system and associated issues are specific functions of the system of interest and the particular discipline associated with that system. The complexity of a system is defined by the level of nonlinearity and the number of variables (or degrees of freedom) of the system. Systems with a small number of degrees of freedom can range from a simple RC circuit, which is a linear, single degree-of-freedom system, to the van der Pol oscillator, a two-degree-of-freedom nonlinear system which exhibits limit cycle oscillations (LCO). Turbulent fluids[13] and real-world structural systems[14] are often characterized by a large number of degrees of freedom and a resultant spatio-temporal complexity. For nonlinear systems, treatment of multiple degrees of freedom and multiple inputs and outputs must be handled appropriately due to potential cross-coupling and energy exchange.[15–17] The analysis of nonlinear fluid dynamics and nonlinear structural dynamics poses a significant challenge for the nonlinear dynamicist. The coupling of these two complex systems into a nonlinear fluid-structure interaction, is, potentially, one of the most complicated problems in nonlinear dynamics.[18]

Nonlinear fluid-structure phenomena may be the result of complex fluid dynamics including shocks, viscous effects, and separated flows. Nonlinear fluid-structure phenomena also may be the result of complex structural dynamics including large deformations and material nonlinearities. A combination of complex fluid dynamics and complex structural dynamics may lead to nonlinear fluid-structure phenomena as well. In order to understand, and therefore predict, these highly complex nonlinear phenomena, computational and experimental methods are being developed and applied.[19] However, computational methods tend to suffer from excessively high computational costs and are not well suited for use in a multidisciplinary, preliminary design environment. Experimental methods rely heavily on traditional linear processes for data analysis, resulting in an inability to measure and, therefore interpret, nonlinear phenomena.

In order to address these challenges, nonlinear sys-

*Senior Research Scientist, Aeroelasticity Branch, NASA Langley Research Center, Hampton, Virginia
†Professor, Engineering Science and Mechanics, Virginia Polytechnic Institute and State University, Blacksburg, Virginia
‡Post-Doctorate Fellow, University of Florida, Gainesville, Florida

tem identification techniques are being applied to problems in unsteady aerodynamics, nonlinear structural dynamics, and aeroelasticity.[19–24] Three system identification techniques currently under investigation are Proper Orthogonal Decomposition (POD), Harmonic Balance (HB), and Volterra theory. This paper discusses recent advances in nonlinear aeroelasticity using nonlinear system identification techniques based on the Volterra theory. Details regarding recent developments and applications of the POD and HB methods can be found in the references.[21] A topic of recent interest is the potential development of hybrid POD/Volterra methods. These hybrid techniques would combine the spatial resolution possible with POD methods with the low dimensionality and computational efficiency of Volterra methods.[21,25]

There are two general categories for system identification techniques: parametric and non-parametric.[26–29] A parametric method assumes a particular model of a system and proceeds to define the coefficients that correspond to that particular model. A non-parametric model seeks to develop the best functional representation of a system based on input-output mappings. Systems also may be classified as being linear or nonlinear, autonomous or non-autonomous, and deterministic or stochastic. It is essential that a system of interest be properly classified as that will determine the method to be used for its identification. The identification of a nonlinear system via the Volterra theory is a non-parametric approach. Additional assumptions associated with the Volterra theory are discussed in the paper.

Experimental investigation of complex flight dynamic and aeroelastic phenomena are best understood by studying the underlying unsteady aerodynamics. To this end, experiments designed to measure the unsteady aerodynamic response of various configurations provide significant and valuable information.[30–33] Experimental results are compared to various types of numerical analyses (such as CFD) to provide insight into the underlying physics of the problem.

Recent applications of the Volterra theory to experimental aerodynamics and aeroelasticity are providing valuable knowledge regarding nonlinear aeroelastic behavior. In particular, the experimental identification of aerodynamic impulse responses may provide insight regarding the dominant flow physics of the experiment as well as an automatic data filtering capability.[34] The application of higher-order spectra (HOS) to flutter data[35] and the identification of Volterra kernels from flight flutter experiments[36–38] are additional examples of this promising application for the Volterra theory.

The goal of this paper is to present a summary of results on recent applications of the Volterra theory to the experimental identification of nonlinear aeroelastic systems. The paper begins with background information and theoretical details of the Volterra theory of nonlinear systems. As part of the experimental identification of nonlinear aeroelastic systems, the identification of unsteady aerodynamic impulse responses from experimental unsteady aerodynamic measurements is presented.[34] The paper presents recent results regarding the application of the Volterra theory, including higher-order spectra (HOS), to wind-tunnel and flight flutter test data. The paper concludes with recommendations for future research.

Volterra Theory

Nonlinear system identification techniques may be applied to problems in nonlinear aeroelasticity in several ways depending on the nature of the nonlinear system under investigation. A nonlinear aeroelastic system may be represented by one of the following combinations of systems: a nonlinear aerodynamic system with a linear structural system (typical of an aeroelastic CFD code such as CFL3Dv6.0); a linear aerodynamic system with a nonlinear structural system (modeling of control surface freeplay for an aircraft flying at subsonic conditions, for example); or a nonlinear aerodynamic system with a nonlinear structural system (large motions of an aircraft flying at transonic conditions, for example). As a result, nonlinear system identification techniques are usually applied to the nonlinear component of these nonlinear aeroelastic systems.

For computational methods, aerodynamic responses can be mathematically isolated from structural dynamic responses. This enables the application of system identification techniques to the nonlinear aerodynamic system, or the nonlinear structural dynamic system, or both. For experimental methods, the measured aeroelastic data may not be easily separated into aerodynamic and structural dynamic components. As a result, the application of system identification techniques to experimental data may result in the identification of nonlinear parameters that are different from the parameters identified for an analogous computational problem. Application of Volterra-based system identification techniques to problems in computational aeroelasticity can result in the identification of aerodynamic Volterra kernels, structural Volterra kernels, or aeroelastic Volterra kernels. Application of Volterra-based system identification techniques to problems in experimental aeroelasticity typically will result in the identification of aeroelastic Volterra kernels. An important exception to this generality would be the measurement of unsteady aerodynamic data using a rigid wind-tunnel model, for example.

In the section that follows, some background information is provided to assist the general reader in understanding the genealogy and variety of applications of Volterra-based methods.

Background

A valuable and important characteristic of the Volterra theory of nonlinear systems is that the theory is well defined in the time and frequency domains for continuous- and discrete-time systems. In particular, this theory has found wide application in the field of nonlinear discrete-time systems[39] and nonlinear digital filters for telecommunications and image processing.[40] However, application of nonlinear system theories, including Volterra theory, to modeling nonlinear unsteady aerodynamic responses has not been extensive. One approach for modeling unsteady transonic aerodynamic responses is Ueda and Dowell's[41] application of describing functions, which is a harmonic balance technique involving one harmonic. Tobak and Pearson[42] apply the continuous-time Volterra concept of functionals to indicial (step) aerodynamic responses to compute nonlinear stability derivatives. Jenkins[43] also investigates the determination of nonlinear aerodynamic indicial responses and nonlinear stability derivatives using similar functional concepts. Stalford et al[44] develop Volterra models for simulating the behavior of a simplified nonlinear stall/post-stall aircraft model and the limit cycle oscillations of a simplified wing-rock model. In particular, they establish a straightforward analytical procedure for deriving the Volterra kernels from known nonlinear functions. Clearly, development and application of Volterra-based concepts depends on the identification of the associated kernels for the problem of interest.

The problem of Volterra kernel identification is addressed by many investigators, including Rugh,[45] Clancy and Rugh,[46] Schetzen,[47] and by Boyd, Tang, and Chua.[48] There are several ways of identifying Volterra kernels in the time and frequency domains that can be applied to continuous- or discrete-time systems. Tromp and Jenkins[49] use indicial (step) responses from a Navier-Stokes CFD code and a Laplace domain scheme to identify the first-order kernel of a pitch-oscillating airfoil. Rodriguez[50] generates realizations of state-affine systems, which are related to discrete-time Volterra kernels, for aeroelastic analyses. Assuming high-frequency response, Silva[51] introduces the concept of discrete-time, aerodynamic impulse responses, or kernels, for a rectangular wing under linear (subsonic) and nonlinear (transonic) conditions. Silva[52] improves upon these results by extending the methodology to arbitrary input frequencies, resulting in the first identification of discrete-time impulse responses of an aerodynamic system. However, potential disadvantages of the Volterra theory include input amplitude limitations related to convergence issues and the need for higher order kernels.[53] It is important, therefore, to develop methods that estimate the highest significant order of a Volterra series kernel representation in order to minimize the amount of computational effort for a given system.[54]

In his dissertation, Silva[53] discusses the fundamental differences between traditional, continuous-time theories and modern discrete-time formulations that allow the identification of discrete-time kernels. The discrete-time methods are then applied to various nonlinear systems including a nonlinear Riccati circuit, the viscous Burger's equation, an aeroelastic wing in transonic flow using a transonic small-disturbance code, and a supercritical airfoil undergoing large plunge motions at transonic conditions using a Navier-Stokes flow solver with the Spalart-Allmaras turbulence model.

With respect to experimental applications, Kurdila et al[55] applied an efficient wavelet-based algorithm to the extraction of the nonlinear Volterra kernels of an aeroelastic system exhibiting limit cycle oscillations (LCO). Recent applications of the Volterra theory to flight test data[36–38] clearly demonstrate the applicability of the Volterra theory to these challenging problems. The experimental identification of aerodynamic impulse responses also has been accomplished recently[34] and the method has demonstrated a valuable data filtering capability. The application of higher-order spectra (HOS), the frequency domain version of the Volterra theory, to nonlinear wind-tunnel flutter data is an example of the potential of these methods as well. There is increased interest in the development of these experimental techniques for use in various experimental settings. The identification of LCO during flight flutter tests is a case in point.

Volterra Theory

The literature on Volterra theory is significant, including several texts.[45,56–58] Discussion of the theory begins by considering time-invariant, nonlinear, continuous-time systems. Of interest is the response of the system about an initial state $\mathbf{w}(0) = \mathbf{W}_0$ due to an arbitrary input $u(t)$ (we take u as a real, scalar input, such as pitch angle of an airfoil) for $t \geq 0$. As applied to these systems, Volterra theory yields the response

$$\mathbf{w}(t) = \mathbf{h}_0 + \int_0^t \mathbf{h}_1(t-\tau)u(\tau)d\tau + \int_0^t \int_0^t \mathbf{h}_2(t-\tau_1, t-\tau_2)u(\tau_1)u(\tau_2)d\tau_1 d\tau_2 + \sum_{n=3}^{N} \int_0^t .. \int_0^t \mathbf{h}_n(t-\tau_1, .., t-\tau_n)u(\tau_1)..u(\tau_n)d\tau_1..d\tau_n. \quad (1)$$

The Volterra series in expression (1) contains three classes of terms. The first is the steady-state term satisfying the initial condition, $\mathbf{h}_0 = \mathbf{W}_0$. Next is the first response term, $\int_0^t \mathbf{h}_1(t-\tau)u(\tau)d\tau$, where $\mathbf{h}_1$ is known as the first-order kernel (or the linear/linearized unit impulse response). This term represents the convolution of the first-order kernel with the system input for times between 0 and t. Lastly are the higher order

terms involving the second-order kernel, $\mathbf{h}_2$, through the n^{th}-order kernel, $\mathbf{h}_n$. The existence of these terms is an indication that the system is nonlinear.[53,59]

The convergence of the Volterra series is dependent on input magnitude and the degree of system nonlinearity. Boyd[60] shows that the convergence of the Volterra series cannot be guaranteed when the maximum value of the input exceeds a critical value, which is system dependent. Of course, the issue of convergence is important, since the Volterra series must be truncated for analysis of practical systems. Silva[53,59] and Raveh et al.[61] consider a weakly nonlinear formulation, where it is assumed that the Volterra series can be accurately truncated beyond the second-order term:

$$\mathbf{w}(t) = \mathbf{h}_0 + \int_0^t \mathbf{h}_1(t-\tau)u(\tau)d\tau + \int_0^t \int_0^t \mathbf{h}_2(t-\tau_1, t-\tau_2)u(\tau_1)u(\tau_2)d\tau_1 d\tau_2. \quad (2)$$

For linear systems, only the first-order kernel is non-trivial, and there are no limitations on input amplitude.

Silva[53] derives the first- and second-order kernels, which are presented here in final form in terms of various response functions:

$$\mathbf{h}_1(t) = 2\mathbf{w}_1(t1) - \frac{1}{2}\mathbf{w}_2(t1), \quad (3)$$

$$\mathbf{h}_2(t1, t2) = \frac{1}{2}\left(\mathbf{w}_1(t1, t2) - \mathbf{w}_1(t1) - \mathbf{w}_1(t2)\right). \quad (4)$$

In (3), $\mathbf{w}_1(t1)$ is the time response of the system to a unit impulse applied at time 0 and $\mathbf{w}_2(t1)$ is the time response of the system to an impulse of twice unit magnitude at time 0. If the system is linear, then $\mathbf{w}_2 = 2\mathbf{w}_0$ and $\mathbf{h}_1 = \mathbf{w}_0$. If the system is nonlinear, then this identification of the first-order kernel captures an amplitude-dependent nonlinear effect. The identification of the second-order kernel is more demanding, since it is dependent on two parameters. Assuming $t2 > t1$ in (4), $\mathbf{w}_1(t2)$ is the response of the system to an impulse at time $t2$ and $\mathbf{w}_1(t1, t2)$ is the response of the system to an impulse at t1 and an impulse at t2. It is clear that, for a linear system where superposition holds, the second-order kernel is identically zero. For a nonlinear system, the second-order kernel can be interpreted as a deviation from superposition, i.e. linear behavior.

Time is discretized with a set of time steps of equivalent size. Discrete time increments are indexed from 0 (time 0) to n (time t), and the evaluation of $\mathbf{w}$ at time n is denoted by $\mathbf{w}[n]$. The convolution in discrete time is

$$\mathbf{w}[n] = \mathbf{h}_0 + \sum_{k=0}^{N} \mathbf{h}_1[n-k]u[k] + \sum_{k_1=0}^{N}\sum_{k_2=0}^{N} \mathbf{h}_2[n-k_1, n-k_2]u[k_1]u[k_2]. \quad (6)$$

where N is the total time record of interest.

It should be noted that an important conceptual breakthrough in the development and application of the discrete-time Volterra theory as a ROM technique is the distinction between a continuous-time unit impulse response and a discrete-time unit impulse response.[53,59] The continuous-time unit impulse response is an abstract function typically defined with an amplitude that reaches infinity while its width approaches zero with an integral equal to unity. This function is difficult, if not impossible, to apply in practical applications (i.e., discrete-time problems). The discrete-time unit impulse response (known as a unit sample response), on the other hand, is specifically designed for discrete-time (i.e., numerical) applications. This function is defined as having a value of unity at one point in time and zero everywhere else. This is clearly a simpler function to implement in a numerical setting. The proof of this and details regarding the very powerful unit sample response can be found in any modern text on digital signal processing.[62]

The identification of linearized and nonlinear Volterra kernels is an essential step in the development of models based on Volterra theory, but it is not the final step. Ultimately, these functional kernels can be transformed into linearized and nonlinear (bilinear) state-space systems that can be easily implemented into other disciplines such as controls and optimization.[21,22,34,45,53,63] Recently, linearized state-space models of an unsteady aerodynamic system have been developed[20] while research into the development of nonlinear state-space models continues.[51]

Higher-Order Spectra (HOS)

The frequency-domain version of the Volterra theory, also known as higher-order spectra (HOS), is simply the Fourier transform of the series shown in (1). Therefore, the Fourier transform of the first-order kernel (for a linear system) is the frequency response function of the system. Higher-order kernels are Fourier transformed into higher-order frequency response functions, referred to as HOS. The primary benefit of these higher-order frequency response functions is that they provide information regarding the interaction of frequencies due to a nonlinear process. For example, bispectra (the frequency-domain version of the time-domain second-order kernel) have been used in the study of grid-generated turbulence to identify the nonlinear exchange of energy from one frequency to another. Linear concepts, by definition, cannot provide this type of information. In addition, some very interesting and fundamental applications using the frequency-domain Volterra theory[64,65] and experimental applications of Volterra methods[66,67] are

providing new "windows" on the world of nonlinear aeroelasticity.

In the recent work by Hajj and Silva,[35,68] the aerodynamic and structural aspects of the flutter phenomenon of a wind-tunnel model are determined via a frequency domain analysis based on a hierarchy of spectral moments. The power spectrum is used to determine the distribution of power among the frequency components in the pressure, strain and acceleration data. The cross-power spectrum, linear coherence, and phase relation of the same frequency components between different signals are used to characterize the bending and torsion characteristics of the model. The nonlinear aspects of the aerodynamic loading are determined from estimates of higher-order spectral moments, namely, the auto- and cross-bispectrum.

For a discrete, stationary, real-valued, zero-mean process, the auto-bispectrum is estimated as[69]

$$\hat{B}_{xxx}[l_1,l_2]=\frac{1}{M}\sum_{k=1}^{M}\left|X_T^{(k)}[l_1+l_2]X_T^{*(k)}[l_1]X_T^{*(k)}[l_2]\right|^2 \tag{7}$$

where $X_T^{(k)}[l]$ is the Discrete Fourier Transform of the k^{th} ensemble of the time series $x(t)$ taken over a time T and M is the number of these ensembles. The auto-bispectrum of a signal is a two-dimensional function of frequency and is generally complex-valued. In averaging over many ensembles, the magnitude of the auto-bispectrum will be determined by the presence of a phase relationship among sets of the frequency components at l_1, l_2, and l_1+l_2. If there is a random phase relationship among these three components, the auto-bispectrum will average to a very small value. Should a phase relationship exist among these frequency components, the corresponding auto-bispectrum will have a large magnitude.[70] Because a quadratic nonlinear interaction between two frequency components, l_1 and l_2, yields a phase relation between them and their summed component, l_1+l_2, the auto-bispectrum can be used to detect a quadratic coupling or interaction among different frequency components of a signal. The level of such coupling in a signal can then be associated with a normalized quantity of the auto-bispectrum, called the auto-bicoherence and defined as

$$b^2_{xxx}[l_1,l_2]=\frac{\frac{1}{M}\sum_{k=1}^{M}\left|X_T^{(k)}[l_1+l_2]X_T^{*(k)}[l_1]X_T^{*(k)}[l_2]\right|^2}{\frac{1}{M}\sum_{k=1}^{M}\left|X_T^{(k)}[l_1]X_T^{(k)}[l_2]\right|^2\ \frac{1}{M}\sum_{k=1}^{M}\left|X_T^{(k)}[l_1+l_2]\right|^2} \tag{8}$$

By Schwarz inequality, the value of $b^2_{xxx}[l_1,l_2]$ varies between zero and one. If no phase relationship exists among the frequency components at l_1, l_2, and l_1+l_2, the value of the auto-bicoherence will be near zero. If a phase relationship does exist among the frequency components at l_1, l_2, and l_1+l_2, then the value of the auto-bicoherence will be near unity. Values of the auto-bicoherence between zero and one indicate partial quadratic coupling.

For systems where multiple signals are considered, detection of nonlinearities can be achieved by using the cross-spectral moments. For two signals $x(t)$ and $y(t)$, their cross-bispectral density function is estimated as

$$\hat{B}_{yxx}[l_1,l_2]=\frac{1}{M}\sum_{k=1}^{M}\left|Y_T^{(k)}[l_1+l_2]X_T^{*(k)}[l_1]X_T^{*(k)}[l_2]\right|^2 \tag{9}$$

where $X_T^{(k)}[l]$ and $Y_T^{(k)}[l]$ are the Discrete Fourier Transforms of the k^{th} ensemble of the time series $x(t)$ and $y(t)$, respectively, over a time T. The cross-bispectrum provides a measure of the nonlinear relationship amongst the frequency components at l_1 and l_2 in $x(t)$ and their summed frequency component, l_1+l_2, in $y(t)$. Similar to the auto-bispectrum, the cross-bispectrum of signals $x(t)$ and $y(t)$ is a two-dimensional function in frequency and is generally complex-valued. In averaging over many ensembles, the magnitude of the cross-bispectrum will also be determined by the presence of a phase relationship among sets of the frequency components at l_1, l_2, and l_1+l_2. If there is a random phase relationship among the three components, the cross-bispectrum will average to a very small value. Should a phase relationship exist amongst these frequency components, the corresponding cross-bispectral value will have a large magnitude. The cross-bispectrum is then able to detect nonlinear phase coupling among different frequency components in two signals because of its phase-preserving effect.

Similarly to defining the auto-bicoherence, one can define a normalized cross-bispectrum to quantify the level of quadratic coupling in two signals. This normalized value is called the cross-bicoherence and is defined as

$$b^2_{yxx}[l_1,l_2]=\frac{\frac{1}{M}\sum_{k=1}^{M}\left|Y_T^{(k)}[l_1+l_2]X_T^{*(k)}[l_1]X_T^{*(k)}[l_2]\right|^2}{\frac{1}{M}\sum_{k=1}^{M}\left|X_T^{(k)}[l_1]X_T^{(k)}[l_2]\right|^2\ \frac{1}{M}\sum_{k=1}^{M}\left|Y_T^{(k)}[l_1+l_2]\right|^2} \tag{10}$$

If no phase relationship exists amongst the frequency components at l_1, l_2 in $x(t)$ and the frequency component at l_1+l_2 in $y(t)$, the value of the cross-bicoherence will be near zero. If a phase relationship does exist amongst these frequency components, the value of the cross-bicoherence will be near unity. Values of cross-bicoherence between zero and one indicate partial quadratic coupling. A digital procedure for computing the auto and cross-bicoherence is given by Kim and Powers[69] and is summarized by Hajj et al.[71]

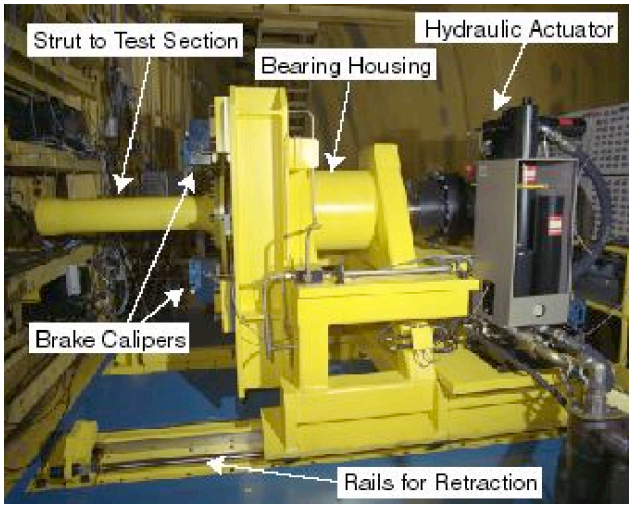

Fig. 1 Side view of the Oscillating Turntable (OTT).

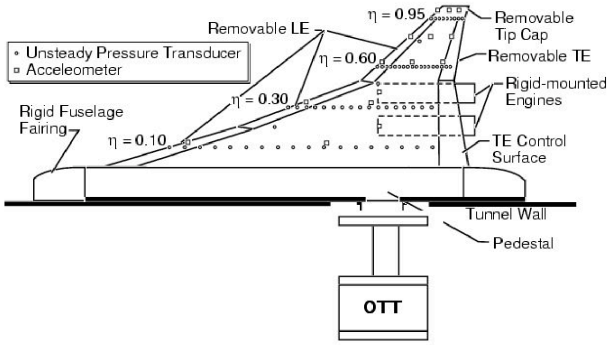

Fig. 2 Planform, model details, and instrumentation layout for the RSM wind-tunnel model.

Description of Experimental Hardware

Oscillating Turntable (OTT)

The OTT is a unique research tool at NASA Langley's Transonic Dynamics Tunnel (TDT) that provides the ability to oscillate relatively large, semispan wind-tunnel models in pitch at frequencies up to 40 Hz. This research tool has been designed specifically for the acquisition of unsteady pressure and loads data on rigid wind-tunnel models in order to study flow phenomena associated with flutter, LCO, shock dynamics, and nonlinear unsteady aerodynamic effects on a wide variety of aerospace vehicle configurations at transonic speeds. Models may be oscillated sinusoidally at constant or varying frequencies, be subjected to a step input, or undergo user-defined motions. It is anticipated that unsteady pressure measurements due to precisely controlled model motions will provide valuable data for CFD correlation and aircraft design with respect to unsteady aerodynamic/aeroelastic phenomena.[31]

Figure 1 highlights key components of the OTT. The OTT utilizes a powerful rotary hydraulic actuator, rated for 495,000 in-lbf, and a digital Proportional, Integral, Derivative, Feedforward (PIDF) control system to position and oscillate models. Power for the OTT is supplied by a 3000 psi, 150 gpm hydraulic power unit which is located outside the tunnel pressure shell.

Rigid Semispan Model (RSM)

The RSM planform is a 1/12th scale configuration based on an early design known as the Reference H configuration that was a component of the High Speed Research (HSR) program. Model airfoil shapes were based on those of the Reference H, with the model wing thickness being increased to a constant 4% thickness-to-chord ratio in order to accommodate pressure instrumentation atthe wing tip. The model was designed to be very stiff to allow the measurement of aerodynamic properties with only negligible effects of structural deformations.

Figure 2 shows the planform layout and main components of the RSM including the OTT mount.

The instrumentation layout for the RSM (visible in Figure 2) consisted of 131 insitu unsteady pressure transducers located at the 10, 30, 60, and 95% span stations. Six additional unsteady pressure transducers were installed at the 20% chord station for the 20, 45, and 75% span stations for both upper and lower surfaces. Channels were carved into the foam core to accommodate the wiring for the instrumentation. Instrumentation also included accelerometers installed throughout the wing. The fuselage fairing used for testing the RSM on the OTT was instrumented with unsteady pressure transducers.

A flexible but otherwise identical version of this model, known as the Flexible Semispan Model (FSM), was fabricated and tested in the TDT in the mid-1990's. The FSM encountered flutter that resulted in structural failure of the model. Details regarding the FSM and flutter testing of the FSM can be found in the references.[30] The test data from the flutter test of the FSM is analyzed using higher-order spectra by Hajj and Silva,[35] summarized in a subsequent section of this paper.

Experimental Results

RSM on the OTT

Unsteady pressure measurements were made on the RSM while the model underwent pitch oscillations on the OTT at frequencies from 1 to 10 Hz. In addition, unsteady pressures were acquired during RSM/OTT step inputs in order to provide data to compute aerodynamic impulse responses.

The identification of experimental unsteady aerodynamic (pressure) ROMs can be performed by using the same techniques used to identify the computational

unsteady aerodynamic ROMs. The Volterra theory of nonlinear systems is used as the basis for modeling the linear and nonlinear dynamic response of the unsteady aerodynamic system under investigation, as described in the references.

For the present study, the identification of experimental unsteady aerodynamic impulse responses will be limited to the first-order, or linearized, kernel. It is referred to as a linearized kernel since identification of the kernel (impulse response) may occur about a nonlinear steady-state condition (such as a transonic Mach number). Future research will focus on the identification of the second-order kernel.

The identification of the experimental unsteady aerodynamic impulse responses (first-order kernel) will consist of the deconvolution of a given input/output pair. The input, in this case, is a sequence of positive and negative step inputs in pitch applied using the OTT and the output is any of several measured pressure responses from the wind-tunnel models. Deconvolution is then used to extract the impulse response for the given input/output pair. For the given OTT step input, an impulse response can be identified for each pressure measurement (sensor) on the wind-tunnel model.

Once the impulse response has been generated, convolution is used to predict the pressure response due to sinusoidal inputs in pitch at various frequencies.[34] The measured results are compared to the predicted results (via convolution) to validate the approach.

For the sake of brevity and to demonstrate the feasibility of the method, results are presented for only one pressure measurement located on the upper surface of the RSM at the 60% span location and the 30% chord station. The data was acquired at a Mach number (M) of 0.8, a dynamic pressure (q) of 150 psf, and with the RSM at zero degrees angle of attack.

Figure 3 presents the step pitch input commanded to the OTT and the resultant pressure response at the pressure transducer location mentioned above. Although a theoretical step input consists of an infinite slope where the step occurs, a physically realizable step input, such as that commanded by the OTT, will be limited by the pitch inertia, stress, and load limitations of the model undergoing pitch. As can be seen, a step input that closely approaches a theoretical step input can, in fact, be applied by the OTT.

Using the sequence of step pitch motions of the OTT as the input and the unsteady pressure measurement as the output, deconvolution is applied to identify the unsteady aerodynamic impulse response. Figure 4 presents the time- and frequency-domain versions of the pressure impulse response identified via deconvolution. As can be seen in Figure 4(b), the identified impulse response exhibits significant frequency content, as is to be expected for an impulse response. An analysis of the unsteady aerodynamic impulse responses

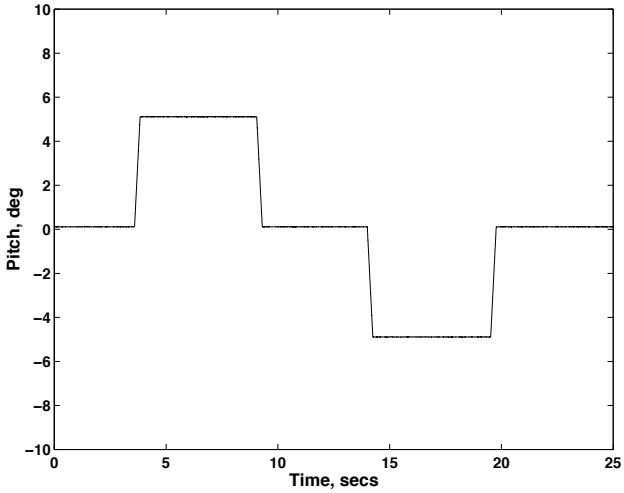

a) Step Input in Pitch

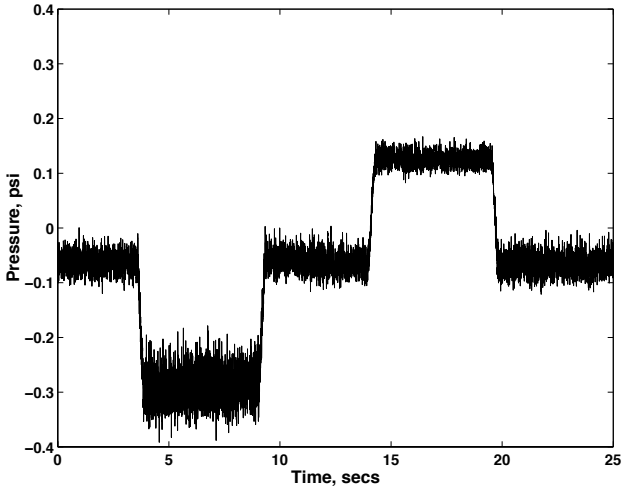

b) Pressure Response due to Step Input in Pitch

Fig. 3 Commanded pitch motion and resultant pressure response on the upper surface of the RSM at 60% span and 30% chord at M=0.8, q=150 psf.

at all pressure transducer locations can provide a spatial mapping of the frequency characteristics of a given configuration at a given test condition. This type of spatial mapping may be useful for the design and optimal placement of various flow control devices.

Upon identification, the unsteady aerodynamic impulse response can then be used to predict the unsteady aerodynamic response due to any OTT input using convolution and the impulse response of Figure 4. In the following figures, comparisons are made between predicted unsteady aerodynamic responses and the measured responses for several sinusoidal OTT motions.

Figure 5 presents the comparison between the measured pressure response and the corresponding predicted pressure response for a commanded oscillation of 1.2 Hz. The comparison is excellent and demonstrates the ability of the method to capture the dom-

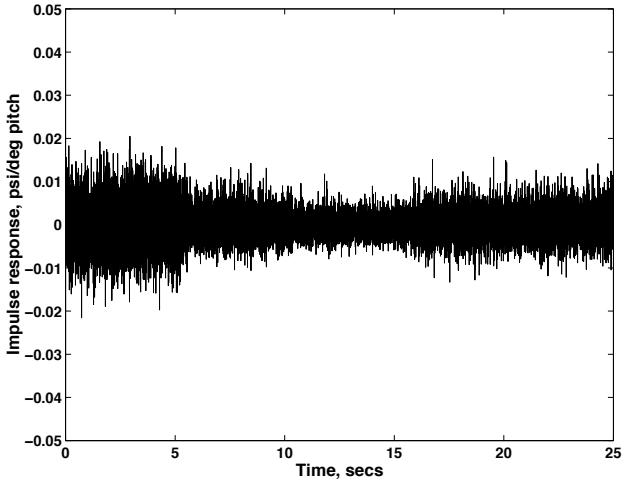

a) Time domain

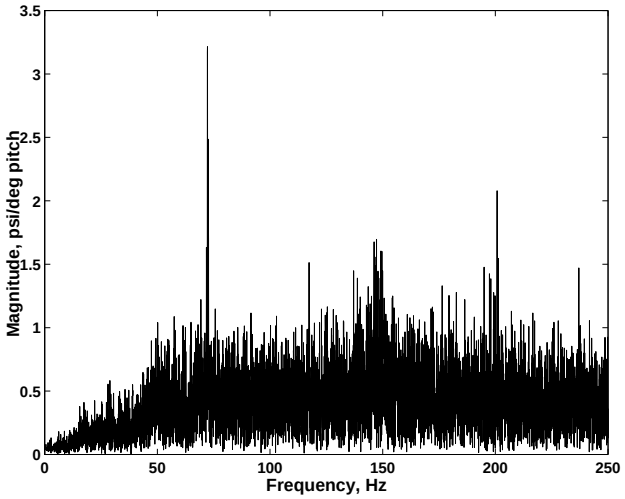

b) Frequency domain

Fig. 4 Pressure impulse response obtained via deconvolution for the RSM; time domain and frequency domain (magnitude).

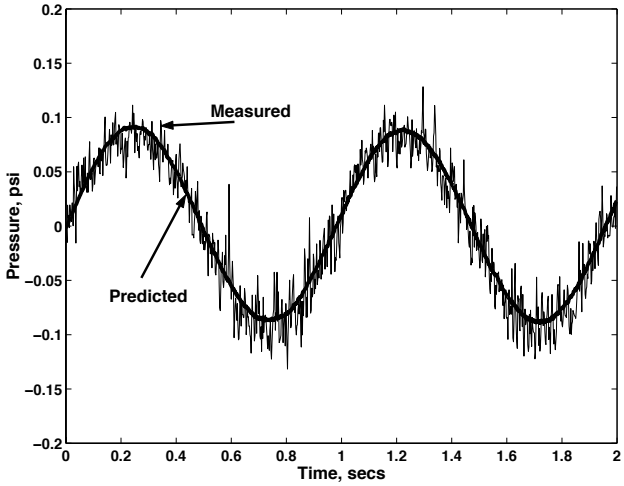

a) Time domain

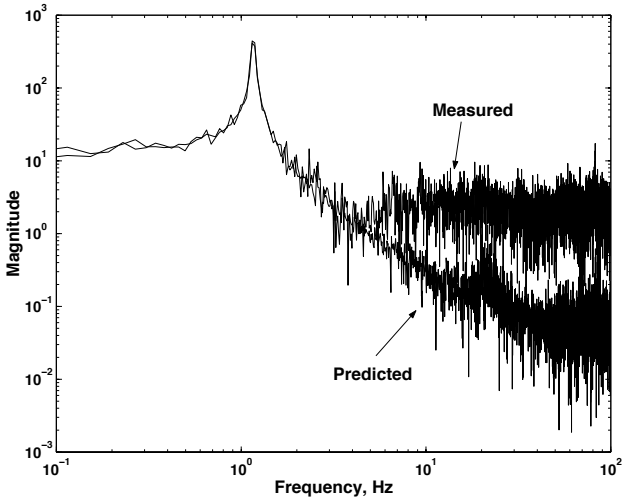

b) Frequency domain

Fig. 5 Measured and predicted pressure responses due to a 1.2 Hz sinusoidal motion of the OTT for the RSM; time domain and frequency domain (magnitude).

inant (driving) frequency while filtering out uncorrelated noise. The deconvolution process automatically identifies the input/output correlations that yield the impulse response. The process of identifying these correlations for a given input/output pair also has the added benefit that it filters out any information that is not correlated to the input. Therefore, uncorrelated measurement noise, for example, is automatically removed as the impulse response is generated. This filtering capability is visible in Figure 5(b).

Figure 6 presents the comparison between the measured pressure response and the corresponding predicted pressure response for a commanded oscillation of 10.0 Hz. For this case, without the predicted response, it would be very difficult to discern any periodicity in the measured response. The filtering capability of the deconvolution method proves to be essential at this frequency.

At this condition, the linearity of the measured pressure response (for this pressure transducer location) is defined by the excellent correlation between the experimental results and the results computed using linear convolution. If predicted results do not compare well with measured results, this could be an indication that some nonlinear effect has influenced the measured response.

In addition, because deconvolution involves input/output correlation, any uncorrelated white noise (measurement noise) is easily filtered out. Note that for several of the examples presented, the filtering was applied at all uncorrelated frequencies, both low and high frequencies. Simple low-pass or high-pass filters would not be able to match this level of filtering capability and much more sophisticated band-pass filters would have to be introduced. However, even

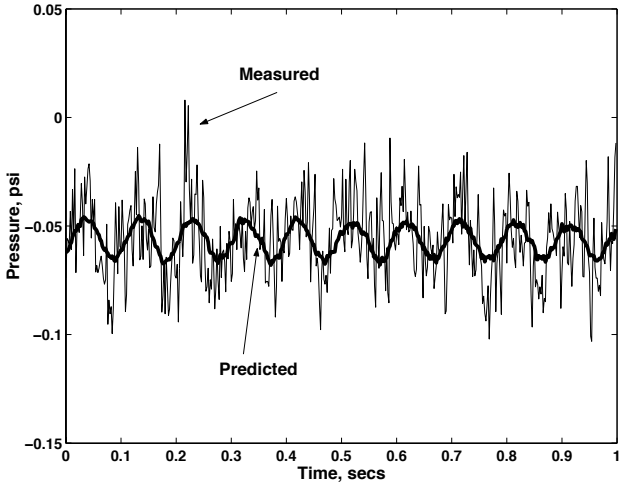

a) Time domain

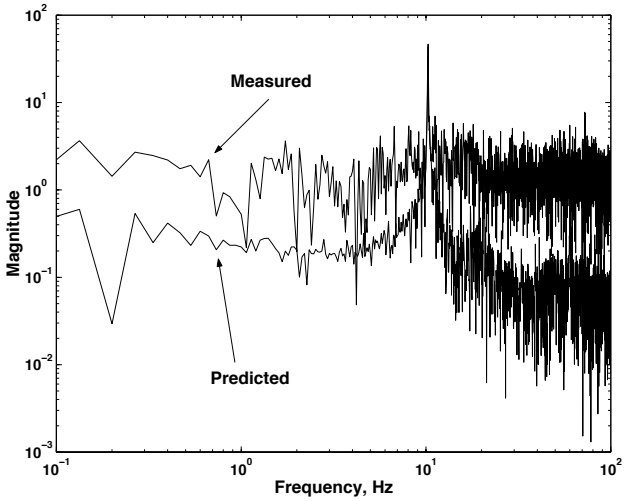

b) Frequency domain

Fig. 6 Measured and predicted pressure responses due to a 10.1 Hz sinusoidal motion of the OTT; time domain and frequency domain (magnitude).

with band-pass filters, the question of which frequency range to filter would remain a serious question for the analyst. Deconvolution automatically handles the filtering without a priori definition of a frequency range where filtering is desired. Analysis of these results can subsequently be used to identify regions of linear and nonlinear behavior which will be helpful in understanding dominant flow physics. Additional results are presented in the references by Silva et al.[34]

Higher-Order Spectra Results

The goal of the effort by Hajj and Silva[35,68] was to identify nonlinear aspects that led to the flutter of an HSCT (High Speed Civil Transport) Flexible Semispan Model (FSM) in experiments conducted at NASA Langley's TDT. The high amplitude responses observed in these experiments present a unique opportunity for detecting nonlinear aspects of the flutter mechanism of this configuration. Of particular interest is a region of high dynamic response that occurred over a broad range of dynamic pressures around a Mach number of 0.98. At the top of this region is a "hard" flutter point that resulted in the loss of the model. The characteristics of the aerodynamic loading and structural strains and motions, as the "hard" flutter is encountered, were determined through analysis of pressure, strain and acceleration data. The nonlinear aspects of the flutter mechanism are identified by using higher-order spectral moments. The use of these moments to investigate limit cycle responses observed on fighter aircraft has been also proposed by Stearman et al.[72]

Analysis of the data indicated the existence of low frequency components that were not related to the modes of the structure. Further insight into the origin and role of these low frequency components, observed primarily in the pressure spectra just prior to the flutter incident, can be obtained from the auto-bispectra of the pressure fluctuations on the upper surface at x/c=0.55 at the 60% span and at x/c =0.80 at the 95% span, shown in Figure 7. At x/c=0.80, the results show a high level of nonlinear coupling between the 0.5 Hz component and the region between 3.0 and 11.0 Hz. This nonlinear coupling has its origin in the flow field and implies that flow structures with these frequencies are coupled. On the other hand, there is no indication of coupling between the 0.5 Hz component and the frequency components observed in the strain gage measurements, namely the 12.7 and the 14.2 Hz components. This suggests that the detected nonlinear effects in the pressure data at these locations are predominantly aerodynamic in nature. The auto-bispectrum at x/c=0.55 at the 60% span station exhibits self coupling at the 0.5 Hz component. Estimates of the auto-bispectrum at other pressure locations did not show nonlinear coupling at the same levels observed at these locations. Yet, it is important to note that, at these locations, the pressure coefficients are relatively large, in absolute sense.

The extent of nonlinear coupling between frequency components at both pressure locations are determined with the cross-bicoherence, shown in Figure 8. The results show that the 0.5 Hz component at x/c=0.55 at the 60% span station is coupled with several components at x/c=0.80 at the 95% span station. This indicates that pressure forces acting at these locations contain nonlinearly coupled frequency components. The importance of these results lies in the fact that this nonlinearity, involving the low frequency components, was only observed in the data acquired as the flutter point was approached, and is associated with the formation of the shock. Moreover, this gives insight into the origin of the low-frequency component observed in the strain gages at these conditions. Although there is still much work to be done, these results are very encouraging.

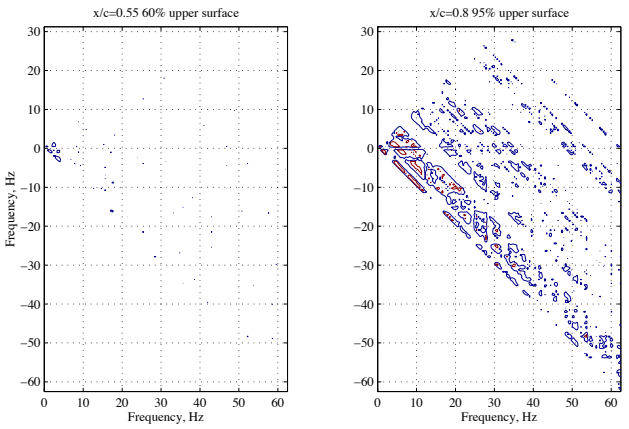

Fig. 7 Auto-bicoherence of the pressure fluctuations at specified chord locations on the upper surface. Contour levels are set at 0.4 and 0.7.

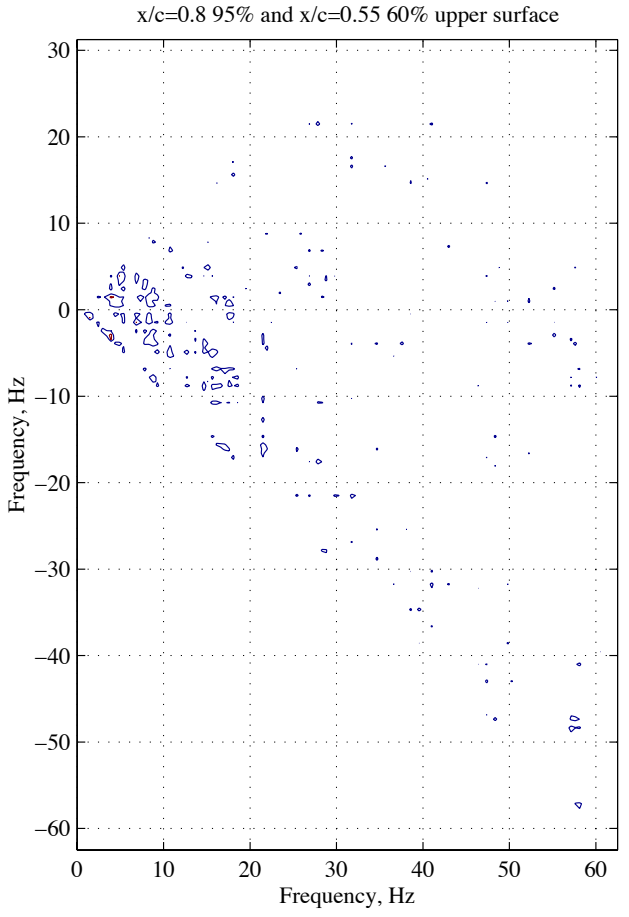

Fig. 8 Cross-bicoherence of the pressure fluctuations at specified chord locations on the upper surface. Contour levels are set at 0.4 and 0.7.

AAW Flight Data Analysis

It is important to mention that, historically, nonlinear Volterra series have not seen widespread use in system synthesis because of the high dimensionality of the higher order, nonlinear terms. This is true from experimental, computational, and analytical perspectives. However, recent work by researchers in multiresolution analysis of the Volterra kernels has shown that the dimensionality of the higher order terms can be significantly reduced. This reduction is due to the fact that wavelet and multiresolution analysis have shown considerable promise for the compression of signals, images, and, in particular, some integral operators. The results by Kurdila et al[66] and Prazenica et al,[67] using experimental pitch and plunge response data from the Texas A & M University's (TAMU) Nonlinear Aeroelastic Testbed (NAT), are excellent examples of this research effort.

Recently, the multiwavelet-based kernel identification algorithm was used to extract Volterra kernels from flight data of the Active Aeroelastic Wing (AAW) vehicle.[36] A wealth of flight data was gathered during subsonic flutter clearance of the AAW. At each flight condition, the aircraft was subjected to multisine inputs corresponding to collective and differential aileron, collective and differential leading edge flap, rudder, and collective stabilator excitations in the range of $3 - 35$ Hz. The results presented herein consider accelerometer data measured during the collective aileron sweeps at the flight condition of Mach number .85 at $10,000$ ft. A single-input/single-output system was considered, with the input taken as the collective aileron position. This collective position was obtained as the average of four position transducer measurements from the right and left ailerons during the sweep. The output was taken as the response of an accelerometer mounted towards the forward of the right wing, just inside the wing fold.

First, second, and third-order Volterra kernels were extracted from the data at each flight condition. The effective memory of the kernels was determined to be 1 sec. in each case. The first-order kernel is represented in terms of 56 multiwavelet coefficients. Taking into account the symmetry of the kernels, the second and third-order kernels are represented in terms of 153 and 969 unique coefficients, respectively. The number of coefficients in the model is directly related to the number of resolution levels retained in the multiwavelet kernel representations. By comparison, for a memory of 1 sec., or 128 samples, a simple discrete-time Volterra model would require 128 first-order coefficients, $8,256$ second-order coefficients, and $357,760$ third-order coefficients, taking the symmetry of the kernels into account.

The filtered collective aileron position and the accelerometer response at a flight condition of Mach .85 at $10,000$ ft are shown in Figure 9. The identi-

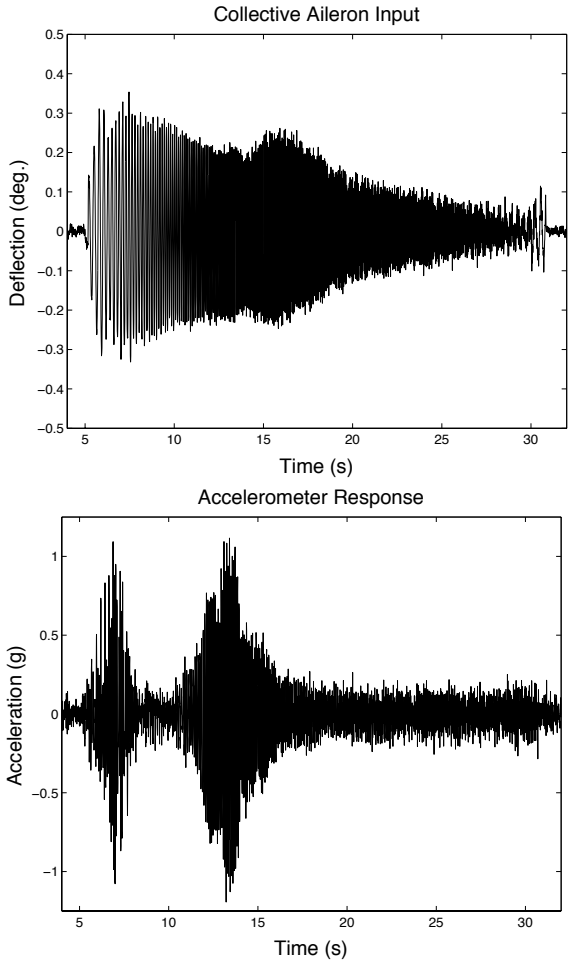

Fig. 9 Collective aileron input and accelerometer response at Mach .85, 10,000 ft.

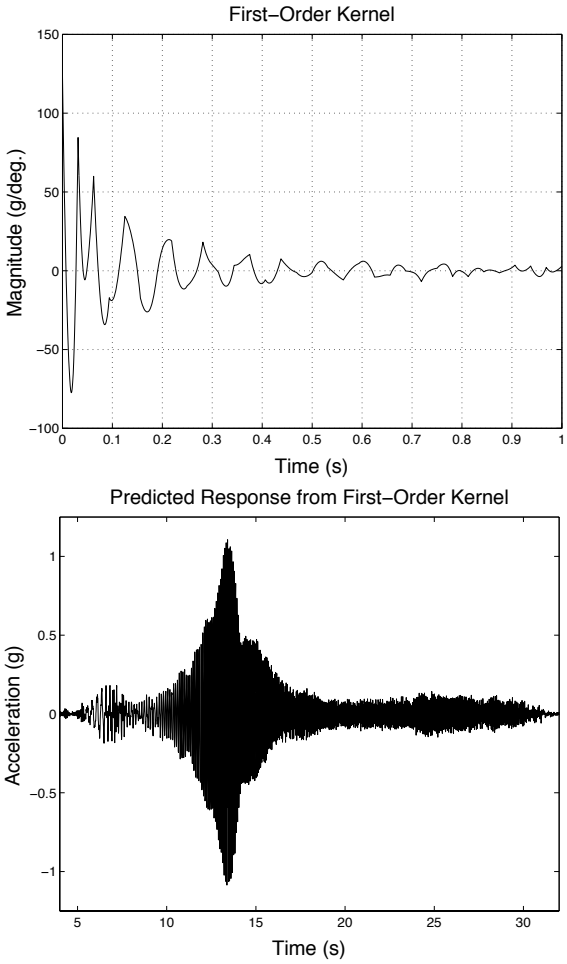

Fig. 10 Identified first-order kernel and predicted response.

fied Volterra kernels and their predicted responses are depicted in Figures 10 through 12. Once again, the response predicted by the first-order kernel is the most dominant, but there is also significant nonlinear response in the $5-10$ sec. range. In this case, the second-order kernel has a small contribution while the third-order response is relatively large. Figure 13 shows the predicted linear response compared to the measured accelerometer response at two intervals in the data set. The predicted linear response matches the measured response well in the $12-14$ sec. range. However, it is clear that the first-order kernel alone cannot account for the nonlinear response in the $7-9$ sec. region. Figure 14 shows the predicted response when the contributions of the second and third-order kernels are included in the model. In this case, the second-order kernel does little to improve the approximation. The addition of the third-order kernel, however, results in a significant improvement in the prediction.

These results indicate that although the first-order kernel captured most of the accelerometer response, it was unable to account for the nonlinear response. The addition of the second-order kernel contributed little to the approximation at this flight condition but the third-order kernel significantly improved the approximation. This research demonstrates the applicability of the Volterra theory to flight flutter data of high-performance aircraft. For additional details, the reader is referred to the reference.[36]

Concluding Remarks

The identification of nonlinear aeroelastic systems based on the Volterra theory of nonlinear systems was presented. Recent applications of the theory to problems in experimental aeroelasticity were reviewed. Discussion of experimental results included the identification of aerodynamic impulse responses, the application of higher-order spectra (HOS) to wind-tunnel flutter data, and the identification of nonlinear aeroelastic phenomena from flight flutter test data of the Active Aeroelastic Wing (AAW) aircraft. The applicability of the Volterra theory to experimental problems in nonlinear aeroelasticity has been demonstrated. The versatility of the Volterra theory, in terms of its applicability in the time and frequency domains, is providing a new tool for the analysis and understanding of nonlinear aeroelastic phenomena.

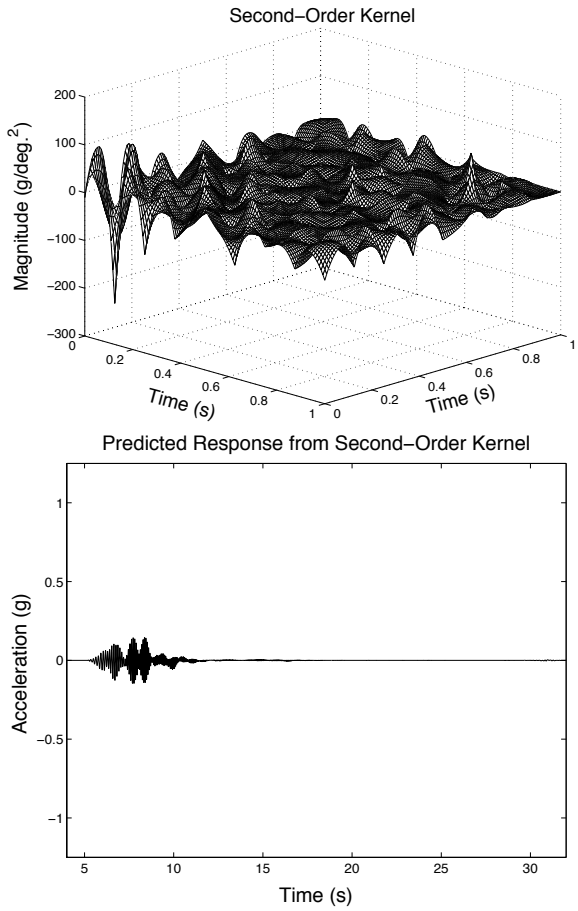

Fig. 11 Identified second-order kernel and predicted response.

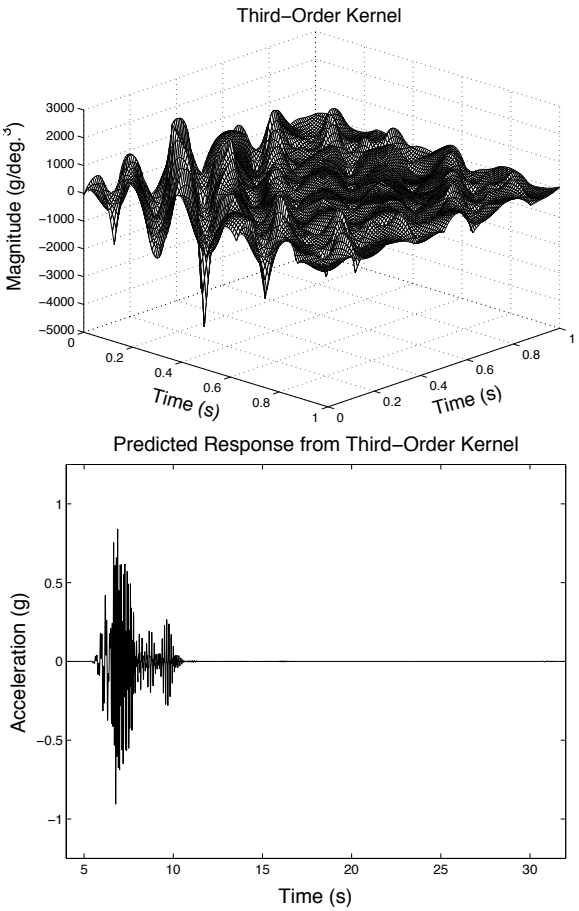

Fig. 12 Identified third-order kernel (one slice at $\gamma = .5$ sec.) and predicted response.

References

[1]Nayfeh, A. H. and Mook, D. T., *Nonlinear Oscillations*, John Wiley & Sons, 1979.

[2]Nayfeh, A. H., *Perturbation Methods*, John Wiley & Sons, 1973.

[3]Moon, F. C., *Chaotic and Fractal Dynamics: An Introduction for Applied Scientists and Engineers*, John Wiley & Sons, 1992.

[4]Seydel, R., *From Equilibrium to Chaos: Practical Bifurcation and Stability Analysis*, Elsevier, 1988.

[5]Khalil, H. K., *Nonlinear Systems*, Macmillan Publishing Company, 1992.

[6]Mohler, R. R., *Nonlinear Systems: Vol. I Dynamics and Control*, Prentice Hall, 1991.

[7]Virgin, L. N., *Introduction to Experimental Nonlinear Dynamics*, Cambridge University Press, 2000.

[8]Strogatz, S. H., *Nonlinear Dynamics and Chaos: With Applications to Physics ,Biology, Chemistry, and Engineering*, Perseus Books, 1998.

[9]Bendat, J. S., *Nonlinear Systems: Techniques and Applications*, John Wiley & Sons, 1998.

[10]Arrowsmith, D. K. and Place, C. M., *An Introduction to Dynamical Systems*, Cambridge University Press, 1990.

[11]Temam, R., *Navier-Stokes Equations and Nonlinear Functional Analysis*, Society for Industrial and Applied Mathematics, 1995.

[12]Brown, R. F., *A Topological Introduction to Nonlinear Analysis*, Birkhauser, 1993.

[13]Mathieu, J. and Scott, J., *An Introduction to Turbulent Flow*, Cambridge University Press, 2000.

[14]Worden, K. and Tomlinson, G. R., *Nonlinearity in Structural Dynamics: Detection, Identification, and Modeling*, Institute of Physics Publishing, 2001.

[15]Thothadri, M., Casas, R. A., Moon, F. C., D'Andrea, R., and C. R. Johnson, J., "Nonlinear System Identification of Multi-Degree-of-Freedom Systems," *Nonlinear Dynamics*, Vol. 32, 2003, pp. 307–322.

[16]Treichl, T., Hofmann, S., and Schroder, D., "Identification of Nonlinear Dynamic Systems with Multiple Inputs and Single Output Using Discrete-Time Volterra-Type Equations," 2002.

[17]Gomez, J. C. and Baeyens, E., "Identification of Multivariable Hammerstein Systems Using Rational Orthonormal Bases," *Proceedings of the 39th IEEE Conference on Decision and Control*, Sydney, Australia, December 2000, pp. 2849–2854.

[18]Dowell, E. H. and Hall, K. C., "Modeling of Fluid-Structure Interaction," *Annual Review of Fluid Mechanics*, Vol. 33, 2001, pp. 445–490.

[19]Dowell, E. H., Edwards, J. W., and Strgnac, T. W., "Nonlinear Aeroelasticity," *44th AIAA/ASME/ASCE/AHS Structures, Structural Dynamics, and Materials Conference*, No. AIAA-2003-1816, Norfolk, VA, 7-10 April 2003.

[20]Silva, W. A. and Bartels, R. E., "Development of Reduced-Order Models for Aeroelastic Analysis and Flutter Prediction Using the CFL3Dv6.0 Code," *Journal of Fluids and Structures*, Vol. 19, 2004, pp. 729–745.

[21]Lucia, D. J., Beran, P. S., and Silva, W. A., "Reduced-Order Models: New Approaches for Computational Physics," *Progress in Aerospace Sciences*, 2004.

[22]Beran, P. S. and Silva, W. A., "Reduced-Order Modeling: New Approaches for Computational Physics," *Presented at the*

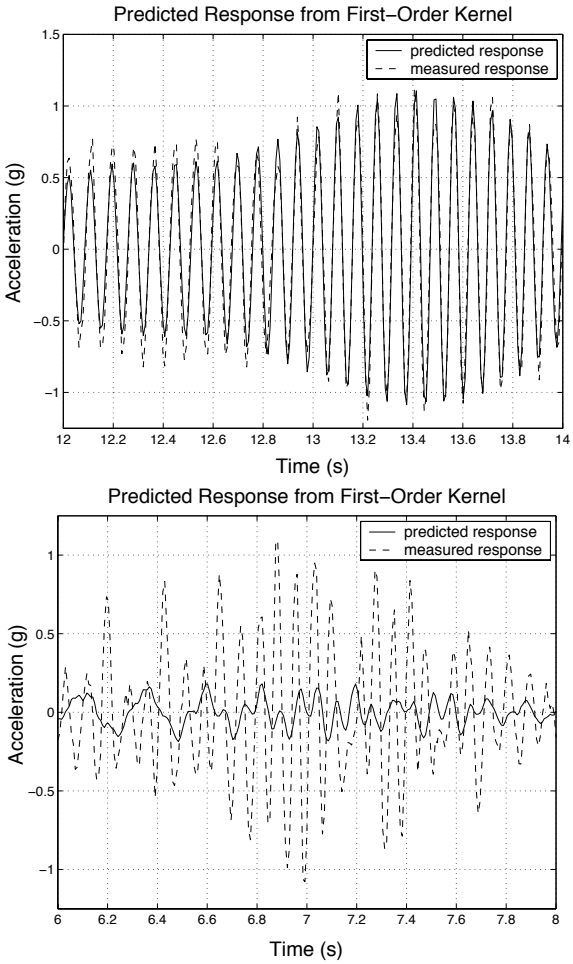

Fig. 13 Predicted response from the first-order kernel at two regions in time.

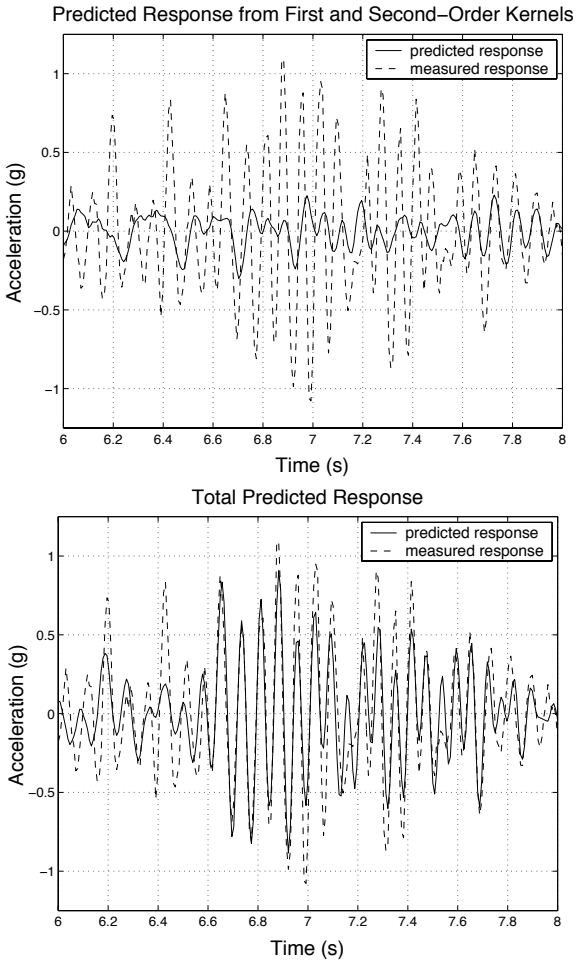

Fig. 14 Predicted response from the first and second-order kernels and the total predicted response of all three kernels.

39th AIAA Aerospace Sciences Meeting, 8-11 January 2001, Reno,NV, January 2001.

[23]Silva, W. A., Beran, P. S., Cesnik, C. E. S., Guendel, R. E., Kurdila, A., Prazenica, R. J., Librescu, L., Marzocca, P., and Raveh, D., "Reduced-Order Modeling: Cooperative Research and Development at the NASA Langley Research Center," *CEAS/AIAA/ICASE/NASA International Forum on Aeroelasticity and Structural Dynamics*, June 2001.

[24]Epureanu, B. I., "Time-Filtered Limit Cycle Computation for Aeroelastic Systems," *AIAA Atmospheric Flight Mechanics Conference and Exhibit*, No. AIAA-2001-4200, Montreal, Canada, 6-9 August 2001.

[25]Lucia, D. J., Beran, P. S., and Silva, W. A., "Aeroelastic System Development Using Proper Orthogonal Decomposition and Volterra Theory," *Proceedings of the 44th Structures, Structural Dynamics and Materials Conference*, No. 03-1922, Norfolk, VA, April 2003.

[26]Ljung, L., *System Identification: Theory for the User*, Prentice-Hall, Englewood Cliffs, 1987.

[27]Eykhoff, P., *System Identification*, John Wiley and Sons, London, 1974.

[28]Juang, J.-N., *Applied System Identification*, Prentice-Hall PTR, 1994.

[29]Nelles, O., *Nonlinear System Identification*, Springer, 2001.

[30]Silva, W. A., Keller, D. F., Florance, J. R., Cole, S. R., and Scott, R. C., "Experimental Steady and Unsteady Aerodynamic and Flutter Results for HSCT Semispan Models," *AIAA/ASME/ASCE/AHS/ASC 41st Structures, Structural Dynamics, and Materials Conference*, No. 2000-1697, April 2000.

[31]Piatak, D. J. and Cleckner, C. S., "A New Forced Oscillation Capability for the Transonic Dynamics Tunnel," *40th Aerospace Sciences Meeting and Exhibit*, Reno, NV, Jan. 2002.

[32]Murphy, P. C. and Klein, V., "Estimation of Aircraft Unsteady Aerodynamic Parameters from Dynamic Wind Tunnel Testing," *AIAA Atmospheric Flight Mechanics Conference and Exhibit*, No. 01-2975, Montreal, Canada, Aug. 2001.

[33]Scott, R. C., Silva, W. A., Keller, D. F., and Florance, J. R., "Measurement of Unsteady Pressure Data on a Large HSCT Semispan Wing and Comparison with Analysis," *Proceedings of the 43rd AIAA/ASME/ASCE/AHS/ASC Structures, Structural Dynamics, and Materials Conference*, No. 02-1648, Denver, CO, April 2002.

[34]Silva, W. A., Piatak, D. J., and Scott, R. C., "Identification of Experimental Unsteady Aerodynamic Impulse Responses," *Proceedings of the 44th Structures, Structural Dynamics and Materials Conference*, No. 03-1959, Norfolk, VA, April 2003.

[35]Hajj, M. R. and Silva, W. A., "Nonlinear Flutter Aspects of the Flexible HSCT Semispan Model," *Proceedings of the 44th Structures, Structural Dynamics and Materials Conference*, No. 2003-1515, Norfolk, VA, April 2003.

[36]Prazenica, R. J., Brenner, M. J., and Lind, R., "Nonlinear Volterra Kernel Identification for the F-18 Active Aeroelastic Wing," *International Forum on Aeroelasticity and Structural Dynamics*, No. US-32, Amsterdam, The Netherlands, 4-6 June 2003.

[37]Brenner, M. J. and Prazenica, R. J., "Aeroservoelastic Modeling and Test Data Analysis of the F-18 Active Aeroelastic Wing," *International Forum on Aeroelasticity and Structural Dynamics*, No. US-6, Amsterdam, The Netherlands, 4-6 June 2003.

[38]Lind, R. and Mortagua, J. P., "Extracting Modal Dynamics from Volterra Kernels to Reduce Conservatism in the Flutterometer," *International Forum on Aeroelasticity and Structural Dynamics*, No. US-23, Amsterdam, The Netherlands, 4-6 June 2003.

[39]Diaz, H., *Modeling of Nonlinear Systems from Input-Output Data*, Ph.D. thesis, Rensselaer Polytechnic Institute, 1986.

[40]Pitas, I. and Venetsanopoulos, A. N., *Nonlinear Digital Filters: Principles and Applications*, Kluwer Academic Publishers, 1990.

[41]Ueda, T. and Dowell, E. H., "Flutter Analysis Using Nonlinear Aerodynamic Forces," *Proceedings of the 23rd AIAA/ASME/ASCE/AHS Structures, Structural, Dynamics, and Materials Conference, New Orleans, LA, AIAA Paper 82-0728-CP*, pp. 462–481.

[42]Tobak, M. and Pearson, W. E., "A Study of Nonlinear Longitudinal Dynamic Stability," NASA Technical Dissertation R-209.

[43]Jenkins, J. E., "Relationships Among Nonlinear Aerodynamic Indicial Response Models, Oscillatory Motion Data, and Stability Derivatives," Proceedings of the AIAA Atmospheric Flight Mechanics Conference, Boston, MA, AIAA Paper 89-3351-CP.

[44]Stalford, H., Baumann, W. T., Garrett, F. E., and Herdman, T. L., "Accurate Modeling of Nonlinear Systems Using Volterra Series Submodels," American Control Conference, Minneapolis, MN, June 1987.

[45]Rugh, W. J., *Nonlinear System Theory, The Volterra-Wiener Approach*, The John Hopkins University Press, 1981.

[46]Clancy, S. J. and Rugh, W. J., "A Note on the Identification of Discrete-Time Polynomial Systems," *IEEE Transactions on Automatic Control*, Vol. AC-24, No. 6.

[47]Schetzen, M., "Measurement of the Kernels of a Nonlinear System of Finite Order," *International Journal of Control*, Vol. 1, No. 3, pp. 251–263.

[48]Boyd, S. P., Chang, Y. S., and Chua, L. O., "Measuring Volterra Kernels," *IEEE Transactions on Circuits and Systems*, Vol. CAS-30, No. 8, August 1983.

[49]Tromp, J. C. and Jenkins, J. E., "A Volterra Kernel Identification Scheme Applied to Aerodynamic Reactions," AIAA Paper 90-2803, August, 1990.

[50]Rodriguez, E. A., *Linear and Nonlinear Discrete-Time State-Space Modeling of Dynamic Systems for Control Applications*, Ph.D. thesis, Purdue University, December 1993.

[51]Silva, W. A., "Application of Nonlinear Systems Theory to Transonic Unsteady Aerodynamic Responses," *Journal of Aircraft*, Vol. 30, No. 5, September-October 1993, pp. 660–668.

[52]Silva, W. A., "Extension of a Nonlinear Systems Theory to Transonic Unsteady Aerodynamic Responses," AIAA Paper 93-1590, April 1993.

[53]Silva, W. A., *Discrete-Time Linear and Nonlinear Aerodynamic Impulse Responses for Efficient CFD Analyses*, Ph.D. thesis, College of William & Mary, December 1997.

[54]Chiras, N., Evans, C., Rees, D., and Solomou, M., "Nonlinear System Modelling: How to Estimate the Highest Significant Order," *IEEE Instrumentation and Measurement Technology Conference*, Anchorage, AK, 21-23 May 2002.

[55]Kurdila, A., Prazenica, C., Rediniotis, O., and Strganac, T., "Multiresolution Methods for Reduced Order Models for Dynamical Systems," *40th AIAA/ASCE/AHS/ASC Structures, Structural Dynamics and Materials Conference, Long Beach, CA,* AIAA Paper 1999-1263-CP, April 1999, pp. 649–658.

[56]Volterra, V., *Theory of Functionals and of Integral and Integro-Differential Equations*, Dover Publications, Inc., New York, 1959.

[57]Schetzen, M., *The Volterra and Wiener Theories of Nonlinear Systems*, John Wiley & Sons, 1980.

[58]Bendat, J. S., *Nonlinear System Analysis & Identification from Random Data*, Wiley-Interscience, 1990.

[59]Silva, W. A., "Reduced-Order Models Based on Linear and Nonlinear Aerodynamic Impulse Responses," *CEAS/AIAA/ICASE/NASA Langley International Forum on Aeroelasticity and Structural Dynamics, Williamsburg, VA*, June 1999, pp. 369–379.

[60]Boyd, S. P., *Volterra Series: Engineering Fundamentals*, Ph.D. thesis, University of California, Berkeley, 1985.

[61]Raveh, D., Levy, Y., and Karpel, M., "Aircraft Aeroelastic Analysis and Design Using CFD-Based Unsteady Loads," AIAA Paper 2000-1325, April 2000.

[62]Oppenheim, A. V. and Schafer, R. W., *Discrete-Time Signal Processing (Prentice Hall Signal Processing Series)*, Prentice Hall, Englewood Cliffs, NJ, 1989.

[63]Silva, W. A., Hong, M. S., Bartels, R. E., Piatak, D. J., and Scott, R. C., "Identification of Computational and Experimental Reduced-Order Models," *International Forum on Aeroelasticity and Structural Dynamics*, No. US-39, Amsterdam, The Netherlands, 4-6 June 2003.

[64]Marzocca, P., Librescu, L., and Silva, W. A., "Nonlinear Stability and Response of Lifting Surfaces via Volterra Series," *presented at the 20th International Congress of Theoretical and Applied Mechanics, Chicago, IL*, 27 August - 2 September 2000.

[65]Marzocca, P., Librescu, L., and Silva, W. A., "Volterra Series Approach for Nonlinear Aeroelastic Response of 2-D Lifting Surfaces," *presented at the 42nd Structures, Structural Dynamics, and Materials Conference, 16-19 April 2001, Seattle, WA*, 16-19 April 2001.

[66]Kurdila, A. J., Carrol, B., Nishida, T., and Sheplak, M., "Reduced-Order Modeling for Low Reynolds Number Flow Control," *SPIE Conference on Mathematics and Control in Smart Structures, Newport Beach, CA*, Vol. 3667, March 1999, pp. 68–79.

[67]Prazenica, R., Kurdila, A., and Silva, W. A., "Multiresolution Methods for Representation of Volterra Series and Dynamical Systems," AIAA Paper 2000-1754, April 2000.

[68]Hajj, M. R. and Silva, W. A., "Nonlinear Flutter Aspects of the Flexible HSCT Semispan Model," *International Forum on Aeroelasticity and Structural Dynamics*, No. US-39, Amsterdam, The Netherlands, 4-6 June 2003.

[69]Kim, Y. C. and Powers, E. J., "Digital Bispectral Analysis and its Applications to Nonlinear Wave Interactions," *IEEE Transactions of Plasma Science*, Vol. PS-7, 1979, pp. 120–131.

[70]Hajj, M. R., Miksad, R. W., and Powers, E. J., "Fundamental Subharmonic Interaction: Effect of the Phase Relation," *Journal of Fluid Mechanics*, 1993.

[71]Hajj, M. R., Miksad, R. W., and Powers, E. J., "Perspective: Measurements and Analyses of Nonlinear Wave Interactions with Higher-Order Spectral Moments," *Journal of Fluid Engineering*, 1997.

[72]Stearman, R. O., Powers, E. J., Schwartz, J., and Yurkovich, R., "Aeroelastic System Identification of Advanced Technology Aircraft Through Higher-Order Signal Processing," *10th International Modal Analysis Conference*, San Diego, CA, 1992.